Journal of Materials Chemistry A

ARTICLE

Angioplasty Mimetic Stented Ion Transport Channels Construct Durable High-Performance Membranes

Received 00th January 20xx,
Accepted 00th January 20xx

DOI: 10.1039/x0xx00000x

www.rsc.org/

Muhammad A. Shehzad[a,b], Xian Liang[a], Aqsa Yasmin[a,b], Xiaolin Ge[a], Xinle Xiao[a], Yuan Zhu[a], Zijuan Ge[a], Yang Wang[a], Liang Wu[a,*] and Tongwen Xu[a,*]

Polyaniline de-doping and re-doping cycling

The CHN elemental analysis for both the polyaniline emeraldine salt state (PANI-ES) and after its de-doping with ammonia solution (base state, PANI-EB) are given in Table S1†. An almost equal weight percentage (a slight increase) of C and N elements, whereas considerable decrease in H confirms the de-doping (or de-protonation) of the PANI-ES, resulting PANI-EB as shown in Scheme S1a†. Another common visual analysis for the de-doping cycling of PANI stents is change in its color from green (PANI-ES) to blue (PANI-EB) and vice versa after re-doping with H^+SPPO. The similar transitions in color were observed while de-doping and re-doping of the stented membranes.

Electrostatic ionic interactions among the PANI stents, SPPO and the dopants

"Electrostatic ionic bonding" is foundation for the stented ion transport channels, as confirmed using Fourier transform infrared spectroscopy in attenuated total reflection mode (FTIR-ATR). Briefly, overlapping of the characteristic absorptions at 1475 cm^{-1} and 851 cm^{-1}, attributable to the out-of-plane bending of C–H in 1,4-disubstituted benzene rings of SPPO and PANI, into comparatively wider and deeper peaks are indicative for close interaction or uniform distribution of both the polymer phases. In contrast to the FTIR spectra of virgin SPPO, large characteristic absorption at 1170 cm^{-1} for sulfonate groups (SO_3^-) further lends support for successful incorporation of the sulfonate dopants in all the stented membranes (Fig. S2†). Two extra bands at 2926 and 2851 cm^{-1} for doped membranes also provide indication of the dopants, interacting with the polyaniline stents, dispersed within SPPO matrix (see interactions in Scheme S2†). A broad band between 3100 and 3700 cm^{-1},presented at the left side of Fig. S2† is due to –OH and –NH stretch, arising from superficial adsorption of water onto the hydrophilic groups in

[a.] *CAS Key Laboratory of Soft Matter Chemistry, Collaborative Innovation Centre of Chemistry for Energy Materials, Department of Applied Chemistry, School of Chemistry and Materials Science, University of Science and Technology of China, Hefei 230026, China*
[b.] *Advanced Materials and Membranes Technology Center, Department of Polymer and Process Engineering, University of Engineering and Technology Lahore, G.T. Road-54890, Punjab Pakistan*
†Electronic Supplementary Information (ESI) available: Scheme S1 & S2, Fig. S1 – S4, Table S1 – S3, and additional details. See DOI: 10.1039/x0xx00000x

the membranes.[1-3] The spectra broadening is expounding relatively larger adsorption of water onto the stented-sulfonate doped membranes especially $(SIM)_{CSA}$ owing to more hydrophilic sulfonate groups and their uniform distribution within the membrane (Fig. 2h). Briefly, the characteristic IR peaks for SPPO, PANI, and sulfonate dopants support the fabrication of electrostatically strengthened ion transport channels and their systematical self-assembling within the stented membranes which could help boost the saline water desalination performance.

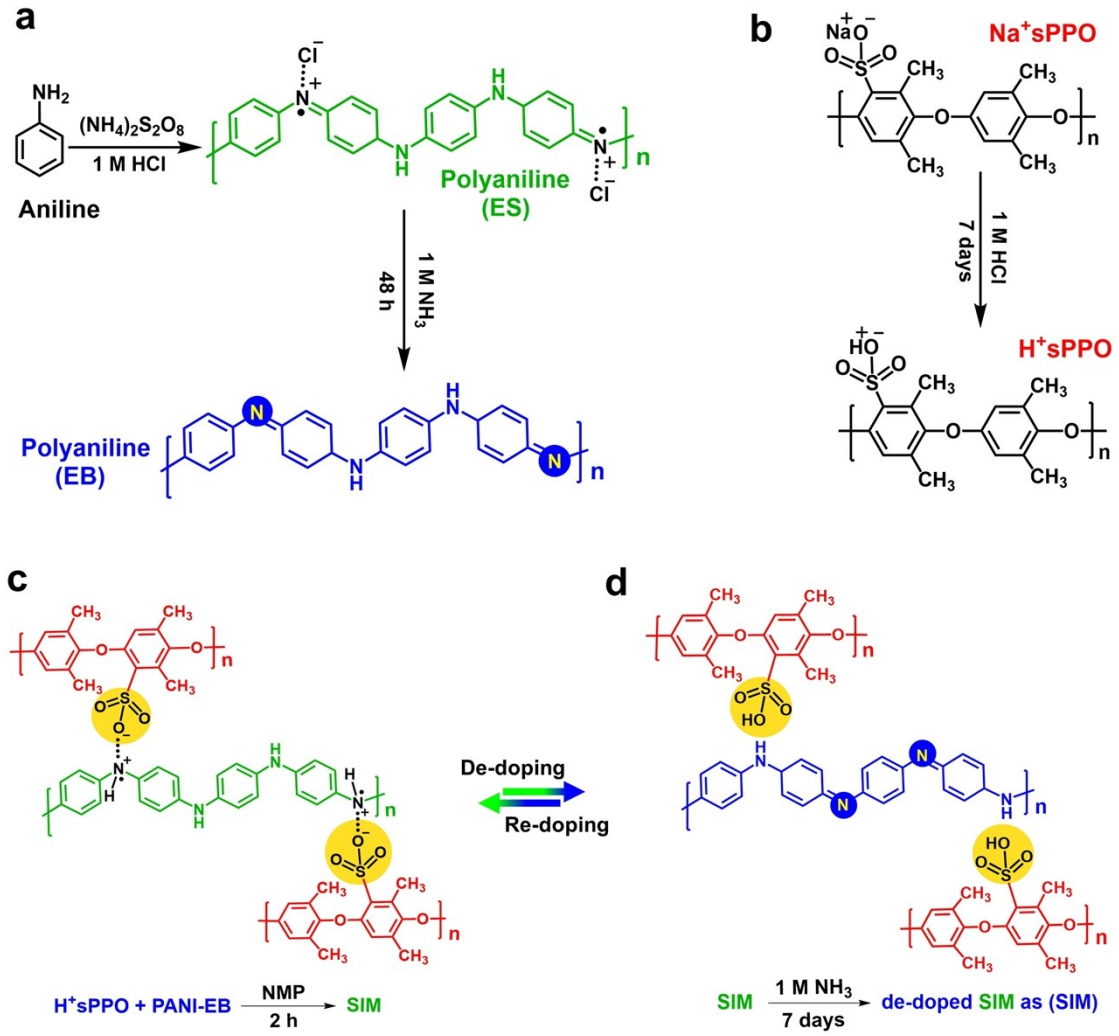

Scheme S1. (a) Synthesis of polyaniline emeraldine base (PANI-EB) as nanostructured stents, possessing the interactable amines. (b) Acidification of the sodium form of sulfonated polyphenylene oxide (Na^+SPPO) as H^+SPPO. (c) Self-assembling of the acid-functionalized SPPO (red) over the PANI-EB stent in such a way as each sulfonic acid group (yellow region, $PPO\sim SO_3^- H^+$) donates its proton to the interactable PANI amine group (N~PANI-EB) and embed over the stent as $PPO\sim SO_3^-\cdots{}^+H\dot{N}\sim$PANI-ES. (d) The PANI de-doping mechanism, whereby liquid ammonia solution alters the positions of the interactable amines.

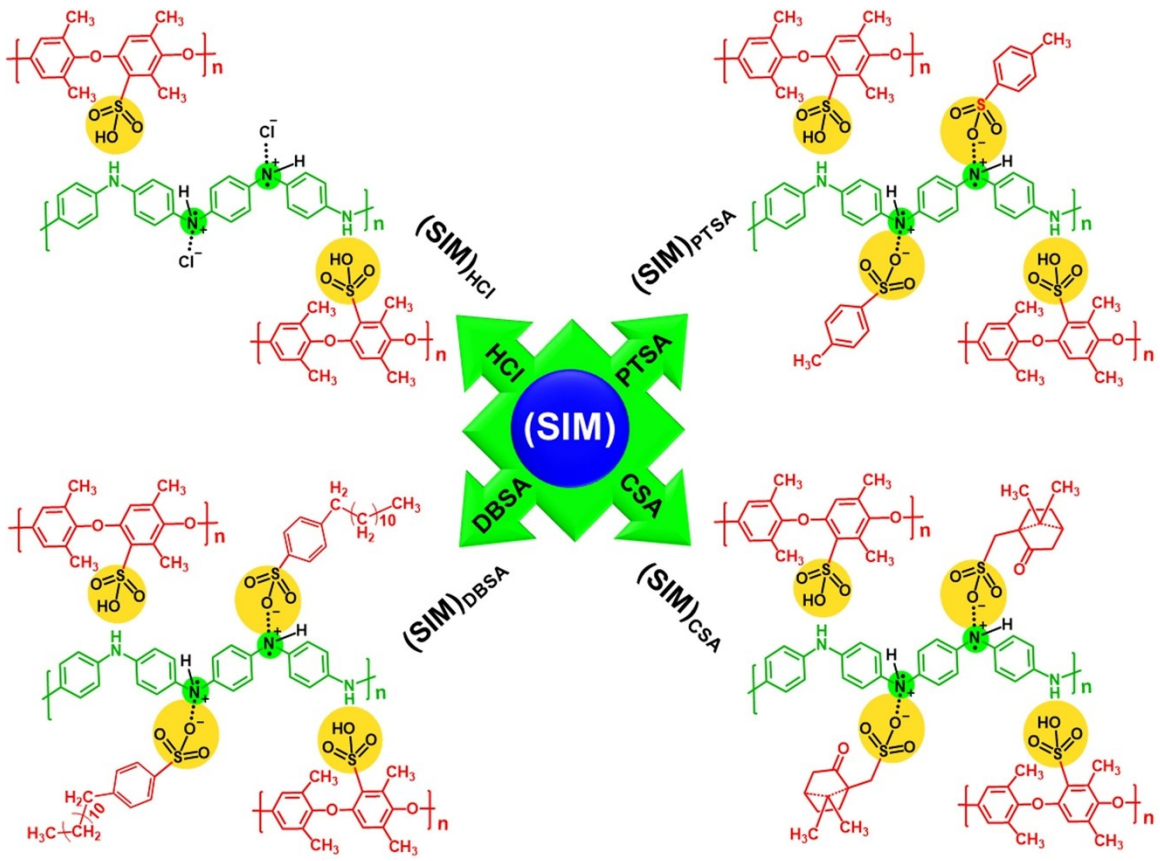

Scheme S2. Schematic representation for re-doping (re-protonation) of the de-doped stented membranes using hydrochloric acid (HCl), dodecylbenzene sulfonic acid (DBSA), para-toluene sulfonic acid (PTSA) and camphor sulfonic acid (CSA), resulting doped stented ion exchange membranes denoted as $(SIM)_{HCl}$, $(SIM)_{DBSA}$, $(SIM)_{PTSA}$, and $(SIM)_{CSA}$, respectively.

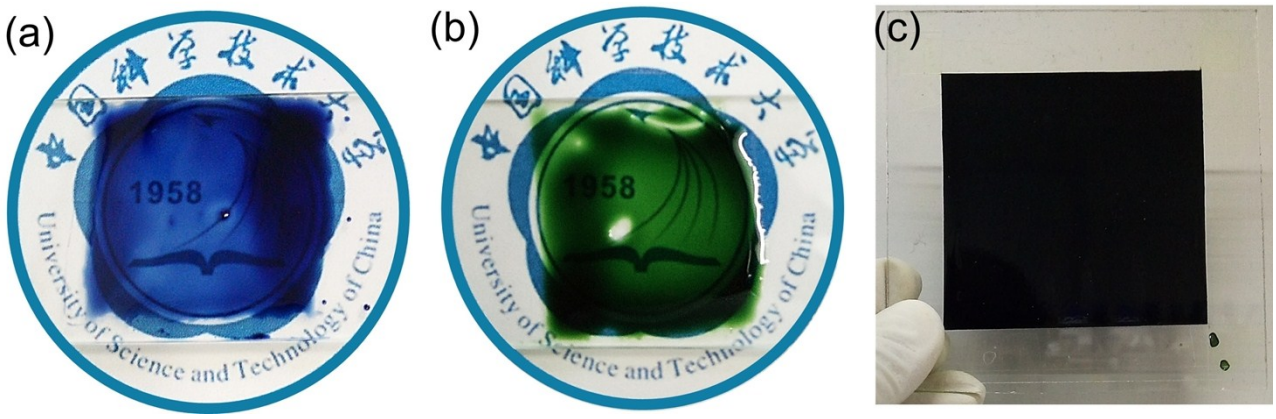

Fig. S1. (a) Blue colored PANI-EB in NMP. (b) Uniformly dispersed and SPPO doped PANI stents. Green color confirms the electrostatic SPPO encapsulation strategy as the SPPO sulfonic acid groups (PPO~$SO_3^-H^+$) donate their protons to the interactable amines of PANI-EB stents (N~PANI-EB) as (PPO~$SO_3^-\cdots{}^+$HN~PANI). Consequently, the acidified SPPO self-assemble over the stents in such a way that all the sulfonic acid groups develop a nanosized hydrophilic layer over the stents (Fig. 3d), which re-dope the blue colored PANI-EB into bright green PANI-ES stents. (c) The dispersant of SITC in Fig. S2b† was cast onto glass plates for preparation of the stented ion exchange membrane.

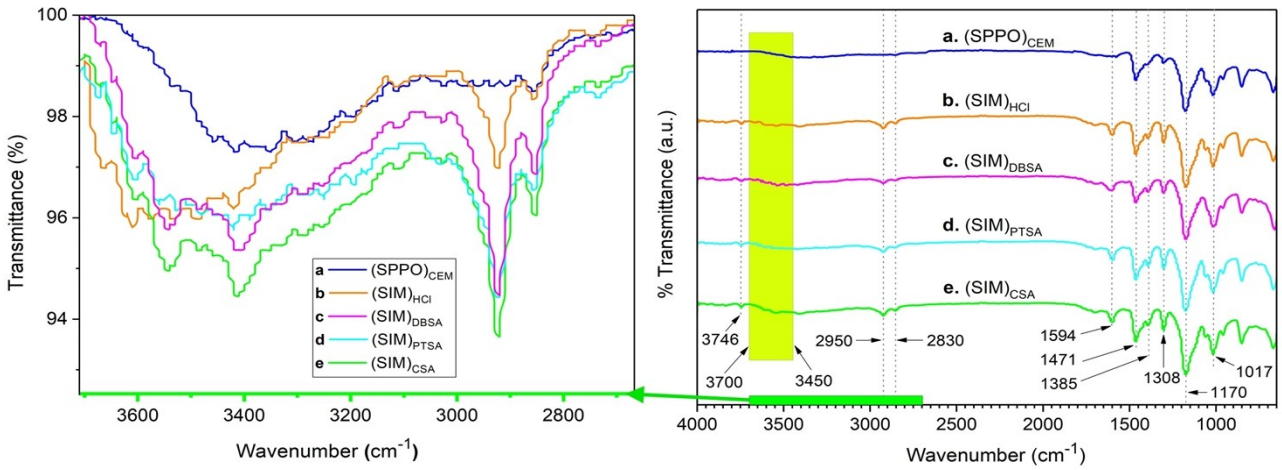

Fig. S2. A comparison between the Fourier Transform Infrared (FTIR-ATR) spectra of **a.** $(SPPO)_{CEM}$, **b.** $(SIM)_{HCl}$, **c.** $(SIM)_{DBSA}$, **d.** $(SIM)_{PTSA}$, and **e.** $(SIM)_{CSA}$ membranes, from 650 to 4000 cm^{-1} wavenumber range. Moreover, zoomed section of the spectra ranging 2700 - 3700 cm^{-1} (left side) shows superficial adsorption for excess of water in the doped PANI membranes, especially the $(SIM)_{CSA}$ membrane which is adsorbing largest water relative to all other membranes.

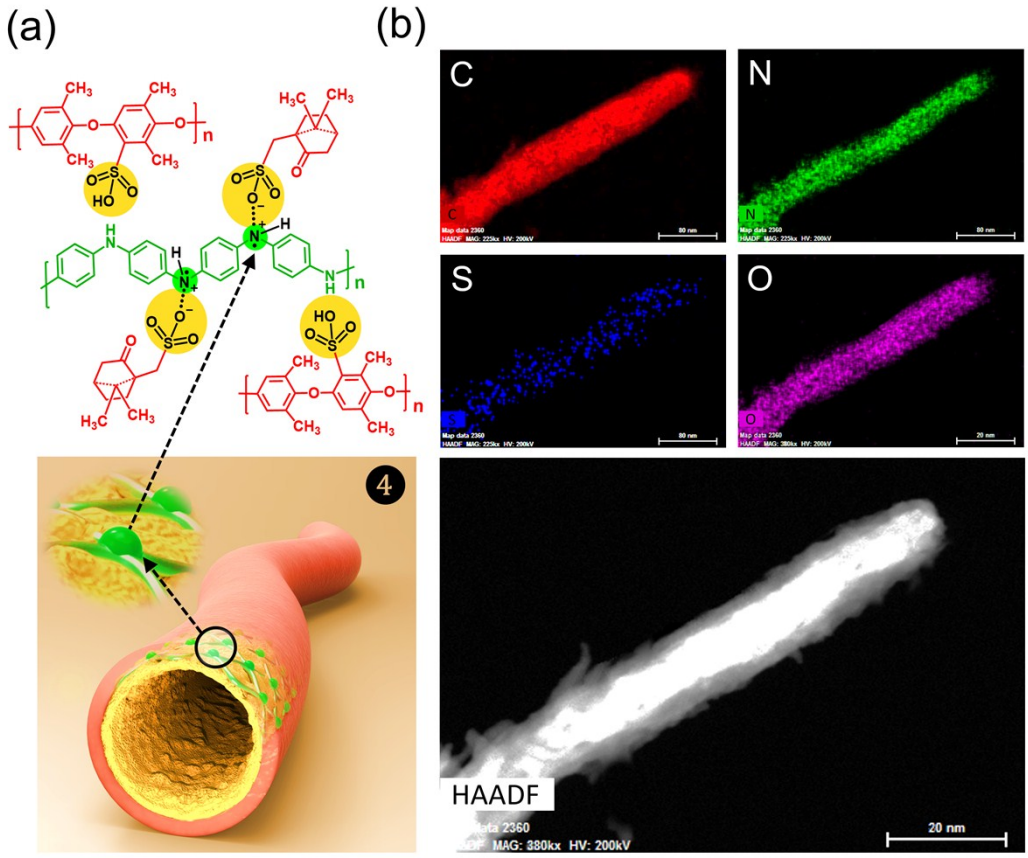

Fig. S3. **Elemental mapping of the stented ion transport channel.** (a) Stage 4 in Fig. 1 shows the stented ion transport channel, where SPPO and CSA dopant are systematically self-assembled at the polyaniline stent (inner network). (b) TEM micrograph of a single stented channel visualizes dark periphery of SPPO and CSA dopant, encapsulating the bright inner stent made of polyaniline. Herein, the TEM mapping displays presence of four elements in the stented channel. Highest concentration of carbon (C), medium of oxygen (O) and lowest of sulphur (S) are in line with the elemental concentration (the chemical structure in Fig. S3a). Moreover, presence of nitrogen (N) indicates polyaniline stent as core of the stented channel (as exhibited in Fig. 2c).

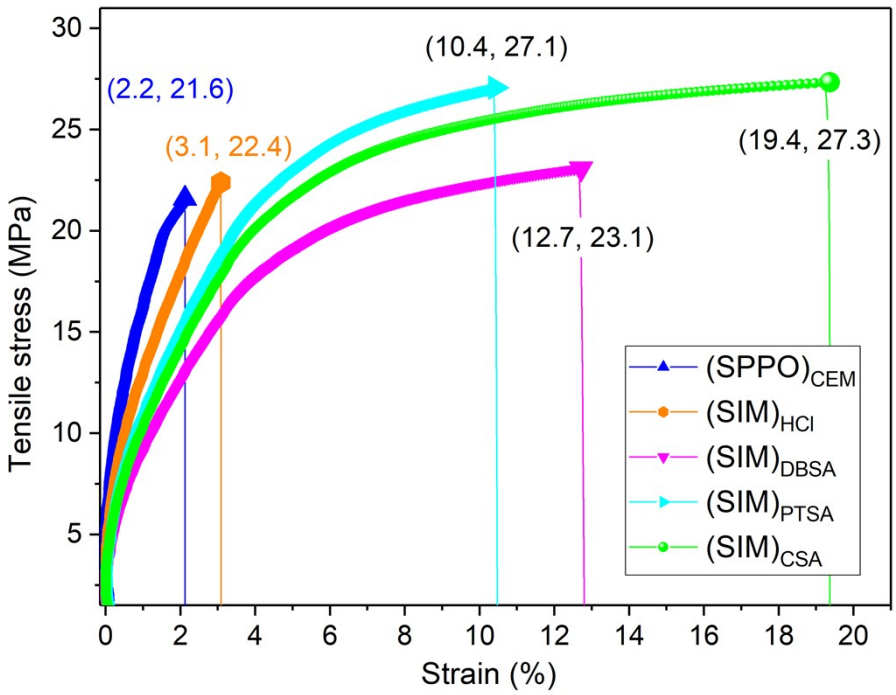

Fig. S4. **Mechanical analysis of the stented membranes.** The plot shows relation between percentage strain or elongation of the membranes (x-axis, %) *vs* tensile stress (y-axis, MPa). Herein, maximum elongation and tensile stress at membrane break are given in plot as (x, y). The curves indicate relatively stiff and brittle nature of the $(SPPO)_{CEM}$ and HCl doped stented membrane $(SIM)_{HCl}$ than the sulfonate doped stented membranes, which is possibly due to the plasticization effect. Therefore, the $(SIM)_{DBSA}$, $(SIM)_{PTSA}$, and $(SIM)_{CSA}$ membranes showed more elongation before break. Particularly, 19.4 % elongation and relatively improved tensile strength (27.3 MPa) of the $(SIM)_{CSA}$ membrane are highly beneficial characteristics for stable electrochemical performance without membrane failure.

Table S1. The elemental analysis for the synthesized polyaniline in both of its emeraldine salt (PANI-ES) and emeraldine base (PANI-EB) states. An almost equal weight percentage of C and N elements but a decrease in H confirms the de-doping (or de-protonation) of the PANI-ES (Scheme S1a†).

Materials	Weight (mg)	N (%)	C (%)	H (%)
PANI-ES	2.630	10.61	56.70	5.36
PANI-EB	2.685	10.76	57.78	4.52

Table S2. Electrochemical characteristics including membrane resistance within linear (ohmic) region (R_O) of the membranes under direct current (DC) stimuli. The testing was performed in 0.5 M NaCl test solution at room temperature (24 ± 1 ^oC) using four compartment electrochemical setup. Analysis for the membranes I-V curves is indicating relatively lower membrane resistance (R_O), higher limiting current density (LCD) values and shorter current plateau lengths (CPL) for the stented membranes compared with the non-stented $(SPPO)_{CEM}$ and commercial $(CMX)_{CEM}$ membranes. Here, OLCD, LV, and OLV are over limiting current density, limiting voltage, and over limiting voltage, respectively.

Membranes	R_O (Ω cm^2)	LCD (mA cm^{-2})	OLCD (mA cm^{-2})	LV (V)	OLV (V)	CPL (V)
$(SPPO)_{CEM}$	6.93	50.1	62.2	0.34	1.12	0.78
$(SIM)_{HCl}$	6.19	68.9	81.4	0.37	0.94	0.57
$(SIM)_{DBSA}$	4.94	72.3	86.9	0.38	0.86	0.48
$(SIM)_{PTSA}$	4.05	76.4	88.5	0.32	0.79	0.47
$(SIM)_{CSA}$	1.83	82.6	97.6	0.16	0.62	0.46
$(CMX)_{CEM}$	4.13	29.3	39.7	0.14	0.65	0.51

Table S3. Comparison for electrochemical characteristics of the fabricated stented ion exchange membrane in this work with the recently published[4-8] and commercial cation exchange membranes[8-13]. Herein, very low electrical resistance (R_0) by the $(SIM)_{CSA}$ indicates comparatively lower consumption of electric energy during saline water desalination process.

Membranes	IEC (meq/g)	Thickness (µm)	Resistance (Ω cm^2)	Remarks
$(SIM)_{CSA}$	< 2.36	69 – 70	< 1.83	Our representative stented CEM
Mixed matrix membrane[4]	> 1.7	60 – 70	< 6.5	Filled with zeolite nanoparticles
PVC-$CuFe_2O_4$ membranes[5]	1.3 – 1.5	80 – 100	< 4	Modified HCEM
HCEM (4.0 wt% - GONs)[6]	1.37	–	6.5 – 7	Containing GO nanoplates
Sulfonic acid membrane[7]	1.93	100	3.25	Polyphenylene oxide polymers
CR61-CMP[8]	2.2 – 2.5	580 – 700	11.0	Ionics Inc., USA
CR67-HMR[8]	2.1 – 2.45	530 – 650	7.0 – 11.0	Ionics Inc., USA
Neosepta CM-2[8]	1.6 – 2.2	120 – 160	2.0 – 4.5	Tokuyama Co., Japan
Nafion N-117[9]	0.9	183	1.5	DuPont Co., USA

Selemion CMV[11]	–	130 – 150	2.0 – 3.5	Asahi Glass Co. Ltd., Japan
TWCED[7,8]	1.4 – 1.6	160 – 180	2 – 4	Tianwei Membrane, China
Morgane CDS[9]	1.7 – 2.2	130 – 170	0.7 – 2.1	Solvay S.A., Belgium
Morgane CRA[9]	1.4 – 1.8	130 – 170	1.8 – 3.0	Solvay S.A., Belgium
Ralex CM-PES[10]	2.2	450	<9	MEGA a.s., Czech Republic
TWCEDI[8]	1.2 – 1.4	160 – 180	5 – 8	Tianwei Membrane, China
Neosepta CMB[12]	–	220 – 260	3.0 – 5.0	Tokuyama Co., Japan
FuMA-Tech, FKS[13]	0.9	90 – 120	2 – 4	FuMA-Tech GmbH, Germany
Aciplex-501SB[11]	–	160 – 200	1.5 – 3.0	Asahi Chemical Industry, Japan

Supplementary references

1. S. L. Zhou, S. S. Mo, W. J. Zou, F. P. Jiang, T. X. Zhou and D. S. Yuan, *Synth. Met.*, 2011, **161**, 1623-1628.
2. S. Zhou, M. Xie, X. Yuan, F. Zeng, W. Zou and D. Yuan, *Am. J. Anal. Chem.*, 2012, **3**, 385.
3. I. Petreanu, D. Ebrasu, C. Sisu and M. Varlam, *J. Therm. Anal. Calorim.*, 2012, **110**, 335-339.
4. S. M. Hosseini, S. Rafiei, A. R. Hamidi, A. R. Moghadassi and S. S. Madaeni, *Desalination*, 2014, **351**, 138-144.
5. S. M. Hosseini, M. Aliabadi Farahani, H. Khalili, B. Van der Bruggen, M. Nemati, Z. Rajabi and A. Ahmadi, *Ionics*, 2019, DOI: 10.1007/s11581-019-02853-5.
6. S. M. Hosseini, E. Jashni, M. Habibi, M. Nemati and B. Van der Bruggen, *J. Memb. Sci.*, 2017, **541**, 641-652.
7. X. Tongwen, Y. Weihua and H. Binglin, *Chem. Eng. Sci.*, 2001, **56**, 5343-5350.
8. X. Tongwen, *J.Memb. Sci.*, 2005, **263**, 1-29.
9. P. Długołęcki, K. Nymeijer, S. Metz and M. Wessling, *J. Memb. Sci.*, 2008, **319**, 214-222.
10. Ralex, Ion exchanges membranes, Product Brochure Mega a.s., Czech Rep.
11. Selemion, Ion exchange membranes Product Brochure Asahi Glass Co., Ltd., Japan.
12. Neosepta, Ion exchange membranes Product Brochure Tokuyama Co., Japan.
13. Fumasep, Ion exchange membranes, Product Brochure FuMA-Tech GmbH, Germany.

